Challenges and Solutions for Fabrication of Magnesium-Based Composites by Friction Stir Processing Technique

P. Sagar[1] and A. Handa[2]

[1]*Ph. D. Research Scholar,*
 I. K. Gujral Punjab Technical University,
 Kapurthala, India
[2]*Department of Mechanical Engineering,*
 I. K. Gujral Punjab Technical University,
 Kapurthala, India

Metal matrix composites (MMCs) are the next-generation materials, globally popular for having numerous potential applications in aircraft, automobile, and biomedical industries. Magnesium is continuously replacing other conventional materials. However, it is a hard to process this material. Recently, friction stir processing (FSP) is drawing attention among researchers to fabricate MMCs. Using the FSP, superior properties of magnesium-based MMCs are successfully achieved. The primary aim of this paper is to review and provide a thorough summary of FSP synthesized magnesium-based composites. Additionally, the effect of secondary-phase particles on the tribological behaviour of produced composite materials is also summed up. Mechanical properties along with microstructural ones produced from stirring process and contribution of strengthening mechanism are addressed too.

Металеві матричні композити (ММК) є матеріалами наступного покоління, широко популярними в усьому світі за численні потенційні застосування в авіяційній, автомобільній і біомедичній промисловостях. Маґній постійно замінює інші звичайні матеріяли. Однак важко обробити матеріял. Останнім часом оброблення фрикційним розмішуванням (ОФР) привертає увагу дослідників до виготовлення ММК. Використанням ОФР успішно досягаються чудові властивості ММК на основі маґнію. Основною метою цієї статті є огляд і надання детального резюме стосовно синтезованих через ОФР композитів на основі маґнію. Крім того, підсумовується вплив вториннофазових частинок на трибологічну поведінку вироблених композитних матеріялів. Також розглядаються механічні властивості поряд з мікроструктурними, що утворюються в процесі розмішування та внеском механізму зміцнення.

1. INTRODUCTION

Metal matrix composite (MMC) are widely known as the cluster of smartly developed engineered materials, synthesized by adding secondary-phase-reinforce micro-, macro- or nanoparticulates with parent materials of different chemical composition [1]. Continuous phase of metal is called matrix, and depending upon the chemical composition of matrix, composites are classified as metal matrix composites (MMCs), ceramic matrix composites (CMC) and polymer matrix composites (PMC) [2]. MMCs recently are drawing interests of the researchers for not only they demonstrate firm bond with reinforced particles also develops no chemical alteration in terms of composition but also exhibits superior properties. MMCs clearly prove themselves as a promising candidate with their wide application in various fields [3, 4]. Copper, magnesium, aluminium and titanium are commonly used matrix materials and TiC, MWCNTs, SiO_2, B_4C and Al_2O_3 few types of reinforced particles. Various manufacturing techniques like diffusion bonding [5], powder metallurgy [6−8], *in situ* fabrication [9], spray deposition [10], stir and squeeze casting [11−14] and vapour deposition been adopted by researchers to fabricate bulk MMCs [15, 16]. All these manufacturing process of developing composites transform material from solid phase to liquid one. On the flip side, techniques, which do not have phase change process like solid-state processing comparatively, shows many merits over conventional phase change techniques. Friction stir processing (FSP) is a newly developed technique based on the principle of friction stir welding (FSW) [17]. Stirring action of FSP been successfully used to disperse secondary-phase particles in the parent metal and producing next generation materials as MMCs [18, 19].

Till now, FSP is widely used to fabricate aluminium-based composites [20−28]. Presently, the world is more concerned about eco-friendly low-emission transportation vehicles with lightweight and maximum-performance. Magnesium been adopted by researchers and scientists over aluminium not for having density two-thirds that of aluminium also for its high strength-to-weight ratio [29]. Magnesium itself or its alloy does not meet the today need. For full filling this purpose, few percentages of particulates need to be added in magnesium or its alloys. Addition of these particulates not only increases the micro-

structure of the composite but also enhanced it mechanical properties. Recently, Sunil *et al.* [30] summarized all work related to magnesium-based composites. This paper present extended study of literature survey and review all recent development in the area of magnesium-based composites' fabrication by FSP. The demanding situations and future bearing of FSP are summed up.

2. SYNTHESIS OF COMPOSITES WITH THE AID OF FSP

FSP in its least difficult structure comprises of a rotating tool that is non-consumable, which is dove into the work piece and afterward moved toward intrigue. The schematic outline of FSP is appeared in Fig. 1.

FSP serves two essential capacities: (a) development of thermal energy, thus deforming work piece material; (b) mixing of secondary-phase particles and form substrate. Intense rubbing of tool with material develop high frictional energy, which results in producing enormous thermal energy. This thermal energy converts the metal into semi-solid phase and makes it softer, while the turning of pin mixes and makes it flow around the pin. It then settles the soft metal depression at the back of the rotating tool. The material that flows around the tool is exposed to serious plastic deformation and heating, which prompts significant dynamic recrystallization, thus refinement of microstructure in the stir zone (SZ) initiated [31].

2.1. FSP Process Variables

FSP machine process variables are classified into five categories. All these are the significant components that direct the successful achievement of the composite manufacture by FSP [32–40]. Varia-
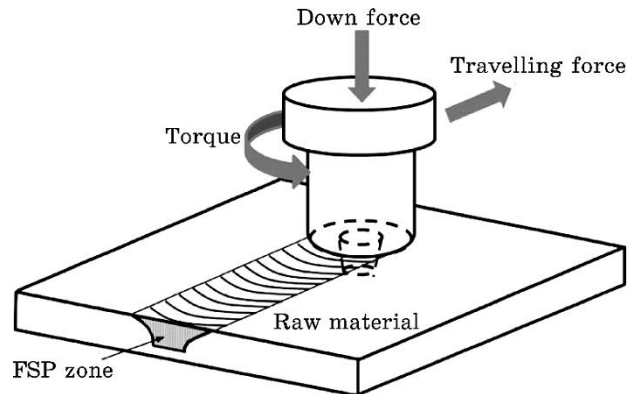

**Fig. 1.** Schematic diagram of FSP technique.
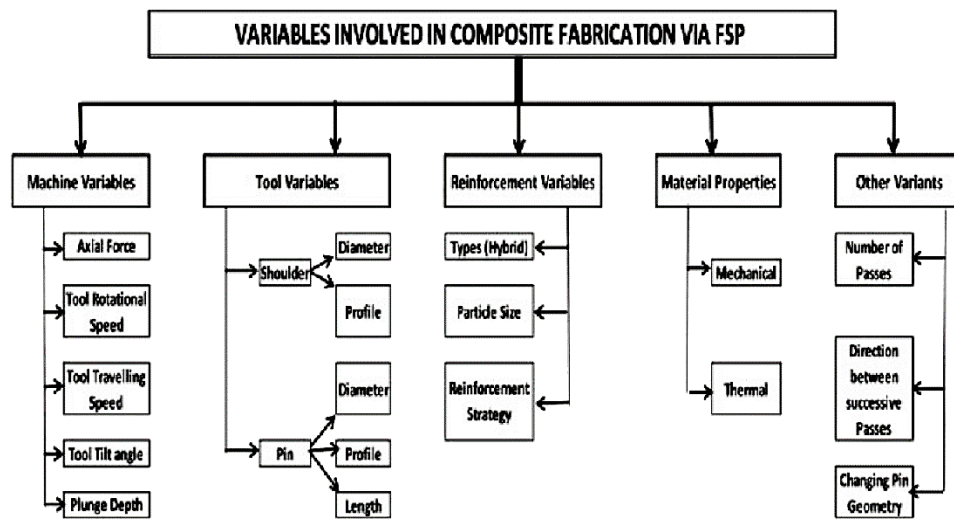
Fig. 2. Various variables involved in FSP [41].

bles are further divided into other various parameters. Figure 2 illustrates a schematic diagram of classification of the variables involved in the manufacture of the composite.

2.2. Doping Method for Reinforced Particles

Prior investigations reveal that formation of composite materials was mainly *via* ceramic slurry layer for FSP process. Now a day's, most common approaches for doping secondary-phase particles into parent metal for composite manufacturing through FSP are shown schematically in Fig. 3. Varity of secondary-phase particles may considered as reported by literature, *i.e.*, TiC, SiC, MWCNT, Al_2O_3, B_4C and SiO_2, *etc.*

Hole Drilling Approach. Holes' filling is a common strategy where required blind holes usually in straight/zig-zag pattern bored on top of the work piece and loaded up with reinforce particles. However, before final experimentation, a pin less FSP tool is employed after loading of reinforced particles to avoid scattering of these particles.

Groove Filling Approach. Groove filling is another common strategy, in which a section is created on work piece and loaded up with reinforce particles. However, before final experimentation, a pin less FSP tool is employed after loading of reinforced particles to avoid scattering of these particles.

Sandwich Approach. In this approach, a layer of reinforced particles is prepared between parent material plates like a sandwich.
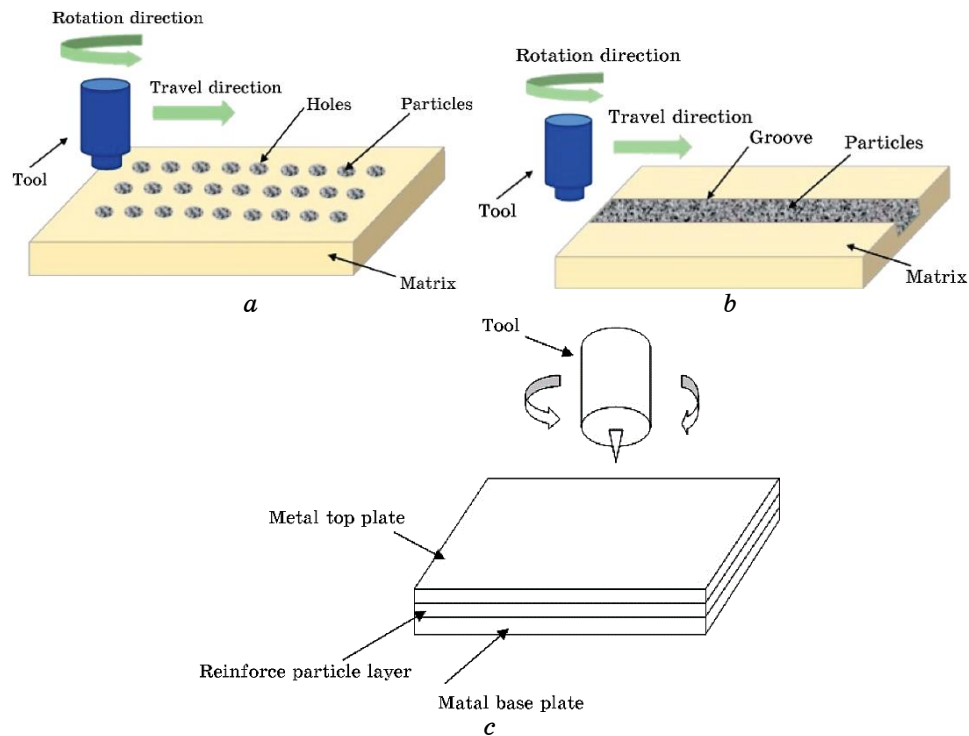
Fig. 3. Schematic diagram of doping approaches [42].

High thermal energy generated by tool breaks the particles and help in fabricating composite. However, uniform distribution may require increased number of passes.

2.3. Tool Geometry

Tool geometry is a vital processing parameter, which generates heat and guide material flow. The shoulder diameter affects heat generation at SZ, and it is usually taken as $D/d = 3$ (where D is shoulder diameter, d is pin diameter) [43]. Common types of tools used in FSP of magnesium-based alloys are presented in Fig. 4.

3. SYNTHESIS OF MAGNESIUM-BASED COMPOSITES WITH THE AID OF FSP

Most common magnesium alloys comprised of aluminium, zinc, thorium and uncommon earth. Using the ASTM alphanumeric designation system encourages grouping magnesium alloys by principal al-
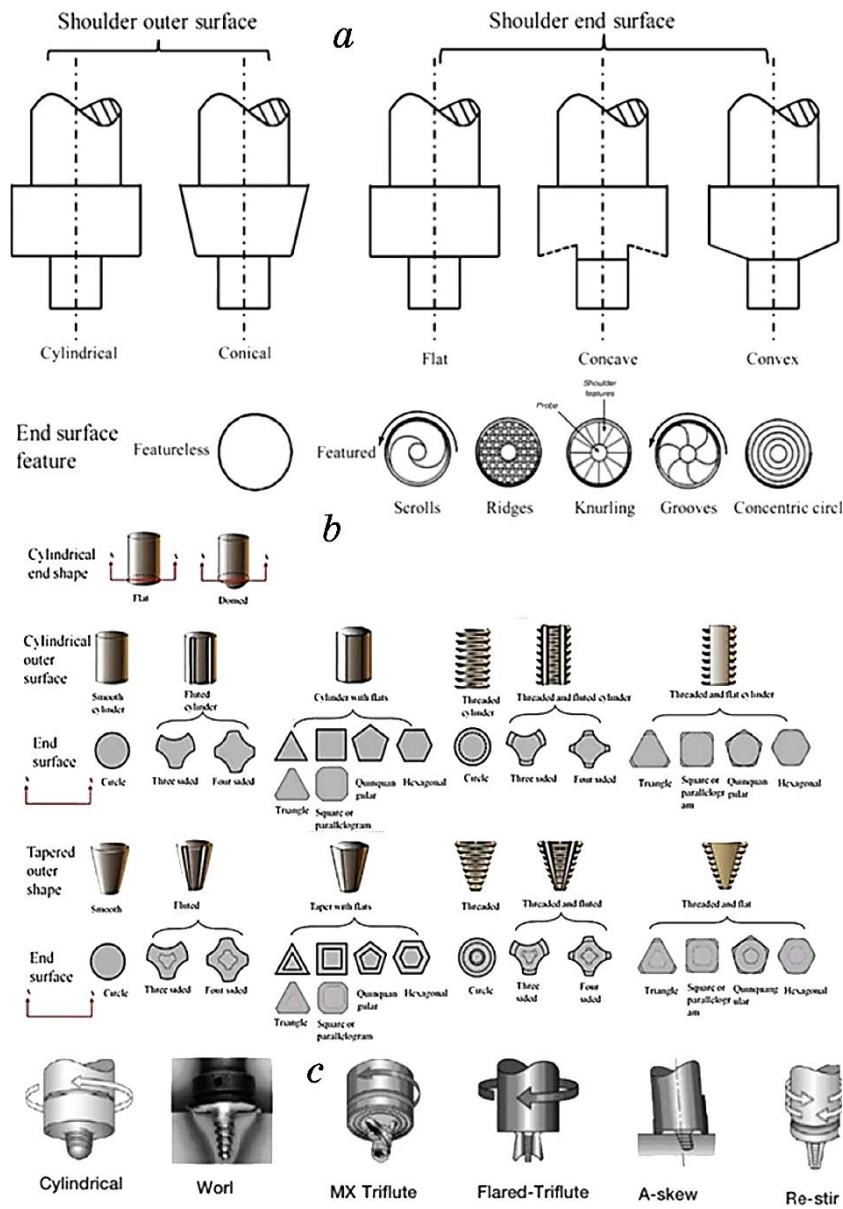
Fig. 4. Common types of tools used for FSP processes **[44]**.

loy composition like Mg–Al–Mn (AM), Mg–Al–Zn–Mn (AZ), Mg–Zr (K), Mg–Zn–Zr (ZK) with rare earth (ZE), Mg–Y–-rare earth metal–Zr (WE). Initial two letters demonstrate the chief code for major alloying components followed by their concentration, respectively. Last alphabet suggests alloy modification [45].

Studies considering major magnesium alloy for composite fabrication *via* FSP, as reported by the literature, are presented here.

3.1. AZ91 Mg Alloy

P. Asadi *et al.* [46] fabricate AZ91/SiC magnesium-based composite considering square tool pin profile with three tool penetration depth (PD) of 0.1, 0.2 and 0.3 mm and a tool tilt angle of 3°. They observed complete cracked processing zone for PD of 0.1 mm, hole and tunnelling cavity for PD of 0.2 mm and sound surface quality for PD of 0.3. They also studied the effect of tool rotational and tool transverse speed on grain size and microhardness by considering groove-filling approach for fabricating magnesium-based AZ91 alloy with 5 μm SiC particles. They consider two 900 and 1400 rpm tool rotational speed and five 12.5, 25, 40, 50 and 63 mm/min tool transverse speeds. Finding of their research work suggests that best result for grain size and microhardness were achieved at tool rotational speed of 900 rpm with transverse speed of 63 mm/min, *i.e.* 7.16 μm and 94 *HV*.

P. Asadi *et al.* [47] further extended their investigation for AZ91/SiC composite and suggested that grain size increases with increase in rotational speed and lowers the microhardness. In addition, it was noted that increasing transverse speed reduced the grain size, while the microhardness increases. It was also added that changing the tool rotation speed resulting in fine grains and uniform distribution of particles.

G. Faraji *et al.* [48] synthesized $AZ91/Al_2O_3$ composite by using friction stir processing. Their work included three different size nanoparticles ranging from nanometer to micrometre scale, *i.e.*, 3000, 300 and 30 nm, and two different tool geometries along with varying number of passes and also studies their effect on performance measures like grain size, cluster size, microstructure and mechanical properties. Findings of their work suggests that grain size in triangular tool is less than square tool but follows opposite trend in case of hardness. Finally, the conclusion drawn from their work suggests that decrease in size of nanoparticle increases hardness of the composite.

D. Khayyamin *et al.* [49] studied the effect of process parameters on microstructural characteristics of $AZ91/SiO_2$ composite fabricated by FSP. They fix tool rotation speed to 1250 rpm, tilt angle to 3° and number of passes to 4 passes with varying transverse speed to 20, 40 and 63 mm/min. They also examine metallurgical and mechanical properties by optical microscopy (OM), scanning electron microscopy (SEM) and Vickers hardness tester. All optical microscopy and scanning electron microscopy tests were conducted on composites having all different passes and different transverse

speed. Outline of the work concluded that grain size decreases, and strength and hardness increase with increase in transverse speed. Increase number of pass increase hardness and reduce grain size.

G. Faraji *et al.* [50] consider tool geometry of two types square and circular to examine the influence of process parameters on AZ91 with and without Al_2O_3 nanoparticles. It can be understood from the work that at tool rotation speed of 900 rpm and transverse speed of 80 mm/min for square tool provides the best result with grain size of 6 μm and microhardness of 103 *HV* as compared to 7.27 μm and 98.52 *HV* without particles.

D. Ahmadkhaniha *et al.* [51] analysed wear resistance on $AZ91/Al_2O_3$ as produced by FSP adopting groove-filling approach with circular tool. They further consider different tool rotation speed, transverse speed and a fixed tool tilt angle of 3° to investigate mechanical and metallurgical properties. Finally, outcome of the study suggests that tool rotation speed of 800 rpm and transverse speed of 40 mm/min give optimum results for grain refinement and wear behaviour.

M. Dadashpour *et al.* [52] introduced 10–15 nm SiO_2 particulates to study the fracture behaviour AZ91C composite fabricated by FSP. H13 tool material was considered along with square pin geometry with a fixed tool rotational speed of 1250 rpm and feed rate of 40 mm/min. Extreme refined grain from starting size of 140 μm to 4 μm was observed along with the hardness of 130 *HV* and ultimate tensile stress of 239.6 MPa for three FSP passes. T. Chen [53] mixed SiC particles and prepared a layer of surface composite on thixoformed AZ91 using the FSP. Wear behaviour of thixoformed AZ91/SiC was compared with thixoformed AZ91 alloy without composite surface. The authors concluded that increasing number of passes could minimize the agglomeration and maximize the SiC particles distribution. Further, they reported reduced coefficient of friction and enhanced wear resistance of surface composite layer when compared with parent alloy. Very recently, N. Singh [54] developed $AZ91/B_4C$ nanocomposite using drill hole approach with cylindrical tool rotating with 900 rpm and having feed of 45 mm/min. Three different sizes of nanoparticles were considered for examination of microhardness and wear behaviour. Finally, study concluded that average hardness, wear resistance increases and wear rate decreases as the reinforce particle size increases.

3.2. AZ31 Mg Alloy

Morisada *et al.* [55] fabricate AZ31 magnesium alloy with SiC *via* using friction stir processing. They used SiC powder of mean diameter 1 μm into a groove of 1 mm×2 mm of a 6 mm thick plate. A

tool of columnar shape of material SKD61 with diameter of 12 mm along with a probe of diameter of 4 mm and length of 1.8 mm was used; also, they fix the value of parameters like tool rotation of 1500 rpm, tool tilt angle of 3° and travel speed of range 25–200 mm/min for processing. OM, SEM and transmission electron microscopy (TEM) tests were conducted to study the microstructural properties of the composite. Findings of the test reported a fine grain size, *i.e.*, 6 μm in the developed AZ31/SiC as compared to the mean grain size, *i.e.*, 79.1, 12.9 of as-received AZ31 and FSP AZ31, respectively, for the travel speed of 50 mm/min. Further, they reported that, as travel speed increases, grain size of the composite decreases. Microvickers' hardness tester with a load of 200 g was used to measure microhardness, and it shows a maximum value of 69.3 *HV* for FSP AZ31 with SiC particles, and 48.1 *HV* and 60.0 *HV* for as-received AZ31 and FSP AZ31, respectively.

Morisada *et al.* [56] studied the influence of addition of multi-walled carbon nanotubes on grain size and hardness of AZ31 magnesium composite prepared through friction stir processing. AZ31 rolled plate of 6 mm thickness with a groove of 1 mm×2 mm, filled with multiwalled carbon nanotubes of outer diameter of 20–50 nm and of 250 nm length were used. A tool of columnar shape of material SKD61 with diameter of 12 mm along with a probe of diameter 4 mm and length of 1.8 mm was used for fabrication. Good dispersion of nanoparticles was observed at 25 mm/min transverse speed and 1500 rpm tool rotation speed, respectively. Hardness of 78 *HV* was observed for AZ31/MWCNT as compared with hardness of 41 *HV* of as-received AZ31.

M. Azizieh *et al.* [57] examine the effect of process parameters like tool profile, rotational speed and number of passes on microstructural and mechanical properties of FSP-fabricated AZ31/Al$_2$O$_3$. They used three kinds of Al$_2$O$_3$ particles with mean diameters of 35 nm, 350 nm and 1000 nm, respectively. Rectangular shape of 60×100×10 mm as cast AZ31 was used along with a groove of 1.2 mm width and 5 mm depth with a grain size of 70 μm. Varying geometry of tools, *i.e.*, tool with a columnar probe without threads, a tool with a columnar probe with threads and a tool with columnar probe with threads and three flutes heat treated till 53 *HRC* hardness along a fixed tool transverse speed of 45 mm/min, tool rotational speed of 800, 1000, 1200 rpm and tool tilt angle of 2° and FSP 2–4 times passes were adopted, and OM, SEM and microhardness tests were conducted to examine the etched sample. Finally, cavity formation was noticed when non-threaded tool was used also they reported that use of threaded pin leads to good grain size along with uniform distribution of nanoparticles. In case of threaded pin with flute, they observed low homogeneity along with tunnelling effect.

M. Azizieh *et al.* [58] synthesized AZ31/Al$_2$O$_3$ composite by using friction stir processing. They considered parameters like rotational speed and number of passes to find out their effect on particle distribution, grain refinement, hardness and temperature changes in the magnesium metal composite. A constant travel speed of 45 mm/min, tool rotational speed of 800, 1000, 1200 rpm, tool tilt angle of 2° and FSP 2–4 times passes were adopted. Temperature in the stir zone was measured by the *K*-type thermocouple immersed in the stir region. Findings suggest that, with increase in tool rotational speed, average grain size, peak temperature and particle distribution increase. In addition, if number of passes increases, nanoparticle agglomeration decreases and hardness increases, which is good. Finally, work concludes that, at 800 rpm, hardness is higher as compared to 1000 and 1200 rpm.

M. Srinivasan *et al.* [59] developed AZ31B/Al$_2$O$_3$ magnesium metal matrix nanocomposites through rotational friction welding. Authors, further examine the influence on mechanical and microstructure for the various controllable parameters like upsetting and friction time, upsetting and friction pressure. Cumulative effect of machine parameters and thermomechanical stresses results in typical grain refinement in the SZ. Authors reported increase in friction time decrease joint efficiency. Microhardness variation is attributed due to distribution of heat produces by friction pressure and time.

C. I. Chang *et al.* [60] synthesized metal matrix magnesium-based composite AZ31/nano-ZrO$_2$ and nano-SiO$_2$ *via* FSP and examined both the microstructure and mechanical properties. A tool with cylindrical probe with shoulder diameter of 18 mm and pin length and diameter of 6 mm with 2° tilt angle along with pin rotation of 800 rpm and advancing speed of 45 min/min was used. Two grooves each of 6 mm in depth and of 1.25 mm in width were cut, in which 10–20 vol.% of nanosize ZrO$_2$ and 5–10 vol.% nanosize SiO$_2$ particles were filled. Mechanical properties like Vickers hardness were checked using a 200-gf load for 10 s along with optical microscopy, scanning and energy dispersive spectrometer, which were conducted to examine mechanical and metallurgical properties. Average grain size of composite produced 4P FSP resulted to be refined up to 2–4 μm.

Y. Huang *et al.* [61] used direct friction stir processing tool, which is hollow and pin less to fabricate AZ31 Mg/SiC*p* surface composite. They used different technique to field the reinforced particles, *i.e.*, through the hole but not only preplaced on it. The reinforced particle directly follows into the through hole for experimentation they adopted constant rotating speed and transverse speed of 400 rpm and 30 mm/min. They also calculated the plunge depth by using equation. Finally, they concluded that SiC-reinforced particles were dispersed homogenously in the stir zone

fabricated by DFSP as compared to FSP. The microhardness of the SZ-fabricated by DFSP increases up to 115.51 *HV*. Moreover, in the wear property test, the low width on the DFSP AZ31 surface with SiC decreases about 210 μm.

M. Balakrishnan *et al.* [62] used magnesium alloy AZ31 with particulates like TiC to fabricate a magnesium matrix composite. They operate, execute or demonstrate the FSP by taking fixed tool rotational speed, transverse speed, and axial force on a 6 mm AZ31 plate by single pass. They engraved four different width (0, 0.4, 0.8, 1.2) and equal depth of 4.5 mm in the plate to introduced varying different fraction of the given (0, 6, 12, 18). Macrostructure and microstructure were studied by digital optical scanner and scanning electron microscope, and it suggested that TiC were properly distributed.

Jiang *et al.* [63] dispersed nano-SiO_2 reinforced by FSP into AZ31 Mg alloy. The main result reflects uniform grain refinement up to less than 1 μm and increase in hardness up to 1.83 times higher than that of the as-received AZ31 can be achieved.

S. Sharma *et al.* [64] fabricated a novel hybrid nanocomposite AZ31/MWCNT−graphene using multipass FSP with constant other parameters. Uniform, refined and more localized grains of average size of 4.0 μm with lesser tensile twin fraction were reported for hybrid nanocomposites as shown in Fig. 5.

Also, uniform dispersion of hybridized reinforce particles leads to significant enhancement of elastic modulus, tensile failure strains along with the improved mechanical properties like microhardness,
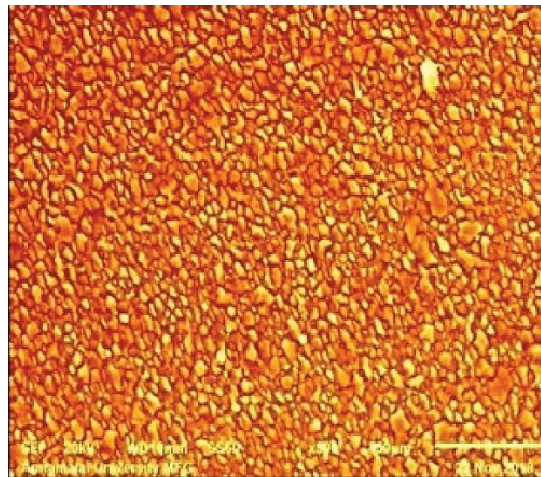

Fig. 5. Microstructure of AZ31Mg−MWCNT−graphene hybrid nanocomposite [64].
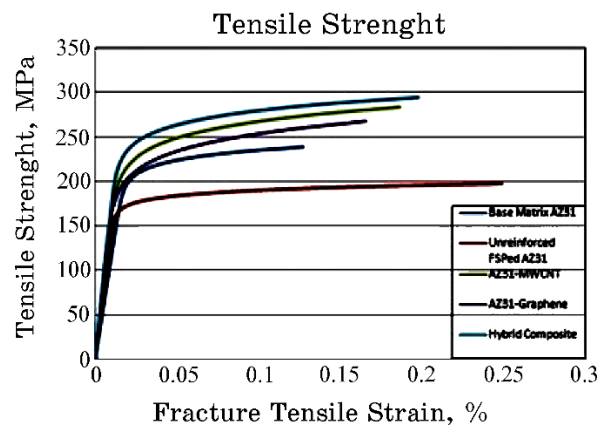
Fig. 6. Tensile strengths of different specimens [64].

i.e., **90.6** *HV* and superior ultimate tensile strength as **49.23%**, as shown in Fig. 6, with yield strength as **32.31%**.

Y. Huang *et al.* [65] execute the process of synthesized AZ31/SiC composite with a special FSP tool unlike other FSP tool. In this novel tool, there are reinforced particles introduced *via* a hole prepared within this new direct friction stir process tool (DFSP). More than four times lesser grain was formed as compared to as cast magnesium alloy grain size of **16.57** μm. Authors further suggested groove or hole filling step can completely be eliminated with new tool also better hardness can be achieved as compared to conventional FSP.

M. Soltani *et al.* [66] synthesized AZ31B/CNT surface composite using FSP. For this research work, authors provide a suitable combination of transverse speed of 24 mm/min and rotational speed of 870 rpm for significant increase in hardness of 60 vickers and reduced grain size of less than 5 μm. M. Navazani and K. Dehghani [67] introduced 5 μm TiC particles for the fabrication of AZ31 magnesium-based composite. Microstructure and hardness of the produced composite were examined. Authors suggested that three vital factors are responsible for dislocation of grain in composite, *i.e.*, dissimilar deformation behaviour between particle and matrix, grain boundaries and thermal expansion. Finally, work suggests that defect free zone can be achieved at 1250 rpm and 50 mm/min with declined grain size.

B. Ratna Sunil *et al.* [68] loaded nanohydroxyapatite-reinforce particles into the groove of base AZ31 magnesium alloy in order to produce composite material. Authors mainly investigate the composite for biomedical applications and degradation of material. Wettability, cytotoxicity and *vitro* bioactivity in supersaturated simulated

field were checked. Grain refinement up to 2 μm was the main reason of enhanced surface energy. Further, authors concluded that dissolution of iron at FSP zone was within tolerance limit, and hence its effect on corrosion is negligible.

Newly, S. Sharma *et al.* [69] examined the influence of tool rotation speeds on mechanical and microstructure properties of fabricated novel hybrid nanocomposite AZ31/MWCNT−graphene using FSP. Optimum ratio of 1.6 vol.% and 0.3 vol.% of MWCNT and graphene was used. Author obtained various values of microhardness at different tool rotation speeds and presented them into a graph form as shown in Fig. 7.

S. Das *et al.* [70] prepared a metal matrix composite WE43/B4C/6 vol.% *via* friction stir processing. For the experimentation work, they used $30 \times 5 \times 1.6$ cm^3 of WE43 plate, B4C of 6 μm along with stepped tool. They drilled a set of holes into the plate for the friction processing and observe the microstructural and mechanical properties through scanning electron microscopy and tensile, hardness tests. Finally, they analyse reduction in grain size and increase in microhardness for four passes as compared to single pass. Further, they concluded that post treatment of composite at 210°C for 48 hours not only increase yield strength from 189−281 but also increase the ultimate tensile strength and elastic modulus with reduction in ductility and elongation to failure. Recently, G. Vedabouriswaran and S. Aravindan [71] introduced boron carbide (B$_4$C), MWCNT and a mixture of $ZrO_2 + Al_2O_3$ secondary-phase particulates for production of magnesium−rare earth alloy−RZ 5-based composite of by single pass FSP. Pinning effect cause by the rein-
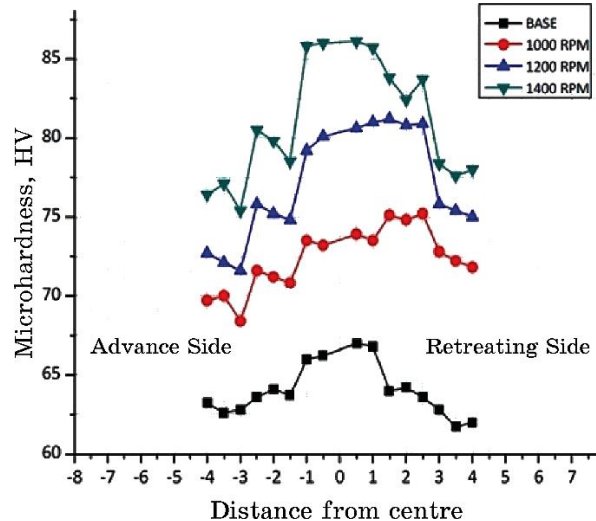

Fig. 7. Range of microhardness at various tool rotation speeds [69].

force particles produces refined grains of range 0.8-to-1.87 μm. Microhardness from 125 *HV* to 403 *HV* was reached with increased ultimate tensile strength with range of 250−320 MPa.

3.3. AZ61 Mg Alloy

J. A. Del Valle *et al.* [72], like C. I. Chang *et al.* [60], used backing plates as of cooper to speed up heat-transfer rate between tool and work piece. They studied the effect of FSP on AZ61 *via* examining mechanical and micro structural properties. Grain refinement was achieved with maximum size of 45 μm to 1.8 μm. Further, authors reported that the surface created during FSP favours basal slip during the tensile test, leading to increase of ductility, a decrease in yield stress and a decrease in strain rate sensitivity in comparison with rolled AZ61 alloy. C. J. Lee *et al.* [73] created AZ61-based nanocomposite by mixing 5−10 vol.% nanosize SiO_2 *via* FSP. Fixing parameters with tool rotation of 800 rpm and tool transverse of 45 mm/min was employed. A back plate for cooling purpose for the whole procedure was deployed beneath. Succeeded FSP, authors declared that as number of passes increases nano-SiO_2 particles turns into a cluster of size going from 0.1 to 3 μm, and the degree of grouping decreases. TEM contemplates that nano-SiO_2 particles stayed as shapeless and opposes change to crystalline stage during whole procedure. X. Du and B. Wu [74] processed magnesium-based AZ61 alloy with rapid heat sink *via* FSP and achieved fine-microstructure at the processed zone with enhanced mechanical properties. Authors observed average grain size less than 300 nm with mean microhardness of 120−130 *HV*, two times higher than that of AZ61 substrate. They further declares that one pass FSP under a high cooling rate may produces ultrafine structure in AZ61 alloy with superior mechanical properties.

3.4. Tribological Behaviour

See Table.

4. STRENGTHENING MECHANISM AND VALUABLE EQUATIONS

Considering the development of magnesium-based metal matrix composites *via* FSP as reported in literature, only selective strengthening mechanism hold good. Grain-boundary and secondary-phase mechanisms are the two strengthening mechanism, and both of them are Hall−Petch relationship and Orowan strengthening.

TABLE. Brief summary of the wear behaviour for magnesium-based composites as reported in literature.

Composite	Tool geometry	Grain size improvement	Machine parameters	Wear test specifications	Significant outcome	References
ZM21/SiC/B$_4$C	Straight cylindrical	40 μm refined up to 20 μm	1200 rpm, 50 mm/min	Pin on disc, load 0.5 kg, sliding speed 640 rpm for 6 km	Wear rate of composite decreases seventy six times to the base metal	G. Madhusudhan Reddy et al. [75]
AZ91/Al$_2$O$_3$/SiC	Straight cylindrical	More refined grains as number of passes increases	730–1800 rpm, 14–80 mm/min with 1–4 passes	Tri-pin on disc, load 50 N, sliding speed 1 mm/s for 500 m	Wear rate decreases as number of pass increases AZ91/AZ91/Al$_2$O$_3$, and Az91/SiC gives almost same wear rate	M. Abbasi et al. [76]
AZ91/TiC	Straight cylindrical	More refined grains	900 rpm, 40 mm/min with PD = 0.3 mm	Pin on disc, load 5–10 N, sliding speed 1 m/s for 2000 m	Wear rate of composite decreases half to the base metal	J. Singh et al. [77]
AZ31/TiC	Straight cylindrical	More refined grains	800 rpm, 40 mm/min	Pin on disc, load 5–20 N, sliding speed 1 m/s for 1.5 km	At 20 N, higher wear resistance was noticed	H. S. Arora et al. [78]
AE42 as cast and FSP AE42	Straight cylindrical	40% reduction in grain size and reached up to 1.5 μm	700 rpm, 60 mm/min	Pin on disc, load 5–20 N, sliding speed 0.3–3 m/s for 2500 m	Higher coefficient of friction attended at low sliding velocities	H. S. Arora et al. [79]

Continuation of **TABLE**.

Composite	Tool geometry	Grain size improvement	Machine parameters	Wear test specifications	Significant outcome	References
As cast Mg/SiC	Threaded cylindrical	Grain size reduced from 170 μm to 3 μm	1300 rpm, 50 mm/min	Pin on disc, load 1–5 kg, sliding speed 1 m/s for 600 m	20% and 47% wear loss was noticed at 1 kg and 5 kg	B. Ram *et al.* [80]
AZ31/Al$_2$O$_3$	Threaded cylindrical	With development of refined grains, hardness increases from 50 *HV* to 90 *HV*	800, 1000, 1200 and 1400 rpm, 45 mm/min and 2° tilt angle	Pin on disc, load 10, 50 and 90 N; sliding velocity 0.12 m/s for 600 m	Wear rate at 1000 and 1200 rpm is higher as compared to 800 rpm	M. Azizieh *et al.* [81]
AZ31/Fly ash	Straight cylindrical	Up to 4 μm grain size achieved	1200 rpm and 40 mm/min	Pin on disc, load 20 N, sliding velocity 1.0 m/s for 3000 m	FSP exhibits 33% lower wear rate as compared to stir cast	I. Dinaharan *et al.* [82]
AZ91/Al$_2$O$_3$	Circular and square tool	Average grain size 5–10 μm was obtained	900–1200 rpm, 40–80 mm/min with 3° tilt angle	Pin on disc, load 50 N, sliding 1.0 mm/min for 500 m	Wear rate decreases more than three times to the base metal	G. Faraji and P. Asadi [83]
AZ31/MWCNT/Al$_2$O$_3$	Cone shape	Much small size grains with microhardness 1.4 times higher than those of AZ31	1050 rpm, 33.4 mm/min	Pin on disc, disc rotation 200 rpm, load 0.65 MPa, 1.30 MPa, 1.95 MPa, 2.60 MPa, 3.25 MPa	For load more than 1.95 MPa, the wear and friction coefficient of hybrid AZ31 composite are low, and it only follows in case of 0.1% Al$_2$O$_3$ and 0.2% CNTs composites	D. Lu *et al.* [84]

Hall–Petch strengthening mechanism has a vital role in the up-gradation of major properties like strength of composites, and its contribution is directly dependent on refined grains existing in metal matrix zone.

The pinning action exerted by the secondary-phase particles gives rise to the concept of grain boundary and grain size, which is further expresses by Zener equation where the grain size of the matrix, d_m, can be achieved [71]:

$$d_m = \frac{4 \alpha d_p}{3 v_p}.$$ (1)

Here, d_p shows particle size; volume fraction of particles is v_p, and α is a constant of proportionality. It may be concluded that newly developed grain size is highly influenced by the size of the reinforcement particles and its volume fraction. Hall–Petch relationship states that hardness is inversely proportional to grain size; in other words, any reduction in the grain size attributes to increase the yield strength. According to Hall–Petch equation (2) and Eq. (3) [85–88],

$$\Delta s_{\text{Hall–Petch}} = K_y \left(d_{\text{composite}}^{-1/2} - d_{\text{matrix}}^{-1/2} \right),$$ (2)

where $d_{\text{composite}}$ and d_{matrix} are the average grain sizes of the composite and matrix, and K_y is the strengthening coefficient,

$$\sigma_y = \sigma_0 + \frac{K_y}{\sqrt{d}},$$ (3)

where σ_y is the yield stress, σ_0 is a materials constant for the starting stress for dislocation movement (or yield strength before FSP), K_y is the strengthening coefficient (a constant specific to each material), and d is the average grain diameter. Based on similar theory [46–47] reported that increases the tool transverse speed, grain size reduces in SZ, which further increases hardness at SZ. The influence of grain size on yield strength of magnesium alloys has also been reported in a number of studies [59, 60, 64 and 70].

M. Azizieh *et al.* [81] and Y. Huang *et al.* [61], based on average grain size uses, further simplified Hall–Petch relationship and used Eqs. (4) and (5) for calculating microhardness of the samples.

$$HV = 43 + 78 d^{-1/2},$$ (4)

$$HV = 40 + 72 d^{-1/2},$$ (5)

where d is the average grain size. Rather, Y. P. Hung [89] estab-

lished a generalized equation

$$HV = 56 + 348d^{-1/2} \qquad (6)$$

for AZ series magnesium alloys. As reported in literature, Fig. 8 shows the ultrarefinement in grain size of magnesium composites as compared to base metal. Figure 9 shows the corresponding values of microhardness for magnesium composites when compared to base metal and.
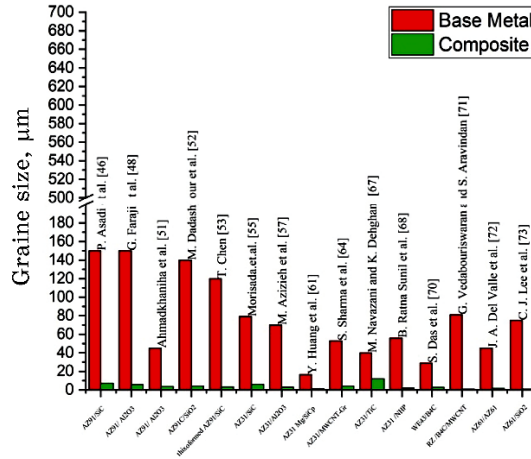
Fig. 8. Comparisons of grain size values for fabricated magnesium-based composites.
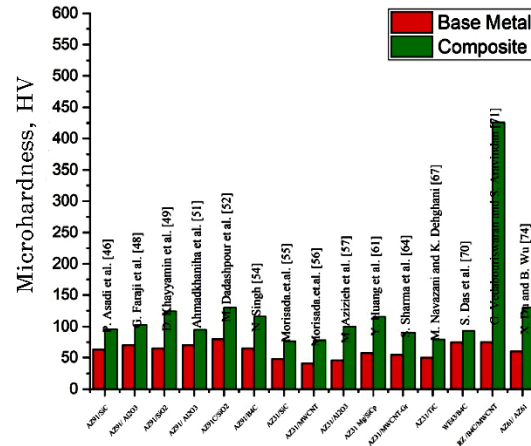
Fig. 9. Enhancement in microhardness for various magnesium-based composites as fabricated *via* FSP.

Orowan strengthening. Z. Zhang and D. L. Chen [90] well explained the contribution of Orowan strengthening mechanism in reinforced metal matrix composites. M. Dadashpour *et al.* [52] concluded that, in fabricating AZ/SiC magnesium-based composite, Orowan strengthening mechanism influences dislocation of grains. G. Vedabouriswaran and S. Aravindan [71] studies the effect of Orowan strengthening mechanism for fabricating magnesium-based composite and concluded insignificant contribution of Orowan strengthening mechanism for their work. S. Sharma *et al.* [69] calculated 58.65 MPa as the total contribution of Orowan strengthening by using Orowan equation as mentioned below in Eq. (7):

$$\Delta s_{\text{Orowan}} = \frac{0.8 G_m M b}{L_p},\qquad(7)$$

where G_m is the shear modulus of alloy matrix, b is the magnitude of Burger's vector of the alloy matrix, and M is Taylor's factor. L_p is the interparticle distance in the composites and can be calculated by equation mentioned below in Eq. (8):

$$L_p = \sqrt{\frac{\pi d_{\text{ref}}^2}{2 V_{\text{ref}}}},\qquad(8)$$

where V_{ref} is the volume fraction of the hybrid reinforcements, and d_{ref} is the average grain sizes of nanocomposites used.

5. DEMANDING SITUATIONS AND FUTURE BEARINGS

Above studies of literature clearly concludes that new materials, especially composite manufacturing, could be effectively achieved *via* FSP. Various reinforcements have been successfully incorporated in metallic matrix by FSP. The grain refinement accomplished by FSP along with high hardness, expanded wear and erosion opposition is the one of a kind point of interest of this procedure. MMCs manufactured by FSP are typically a kind of defect free composites with homogeneous distribution of particles. FSP has indicated promising outcomes in different investigations. Copper, titanium, aluminium, and magnesium materials are the most commonly accepted materials used to supply FSP surface MMCs. Magnesium-based components are among them a category of tough to process materials. It has been unmistakably reported in literature and, in reality, there is a lot of improvement for as long as decade those distinctive magnesium-based surface composites can be effectively delivered by FSP. Furthermore, A. Sanaty-Zadeh [91] studies different strengthening mechanisms, and it is worth maintaining that

Hall−Petch strengthening mechanism is the most important factor, which should not be neglected even in microscale grain.

Apart from various applications of MMCs prepared by FSP yet production, engineers are still wondering for the best outcome of the FSP process. Compound and articulate surfaces are hard to produce by FSP. More FSP passes could only have a homogeneous mixture of the reinforce particles into metal matrix, thereby increasing the cost of output. Tool wear is a significant issue in FSP particularly at high temperature. Hence, tungsten-based tools are highly recommended for FSP processes. These constraints confine the utilization of FSP to process hard surface composites. Flow of the reinforce particles into the matrix is still wide area, which needs to be explore. Optimizing the FSP parameters and developing a model is still an area of future scope.

6. CONCLUSIONS

Literature study clearly summed up that FSP is a potential candidate to produce magnesium-based composites. Mainly two holes filling approach and groove filling approach been adapted for doping the reinforce particles into the metal matrix. Every technique holds its advantages and limitations. Grain refinement, improved hardness, wear opposition, mechanical conduct, improved bioactivity and erosion obstruction are the normal perceptions in the entirety of the magnesium-based composites produced by FSP. The relative contribution of Orowan strengthening effect increases with decreasing size of nanoparticles, and Hall−Petch strengthening mechanism increases with decreasing size of grains.

Dominant part of the work has been done utilizing AZ arrangement magnesium compounds. It is foreseen that composites of other magnesium combinations likewise will be created by FSP in future for a wide scope of uses. Lastly, it is summed up that FSP is a potential candidate to produce magnesium-based composites, and, in future, many more magnesium composites may be produced using FSP.

REFERENCES

1.   William Smith, Javad Hashemi, and Ravi Prakash, *Materials Science and Engineering In SI Units (SIE) Paperback* (McGraw Hill Education: 2017).
2.   T. W. Clyne and D. Hull, *An Introduction to Composite Materials* (Cambridge−New York, NY: Cambridge University Press: 2019); https://doi.org/10.1017/9781139050586.
3.   J. van Suchtelen, *Philips Res. Rep.*, **27**: 28 (1972).
4.   D. D. L. Chung, *Composite Materials Science and Applications* (New York:

Springer: 2010).
5.   I. Mukhin, E. Perevezentsev, and O. Palashov, *Opt. Mater. Express*, **4**, No. 2: 266 (2014); doi:10.1364/ome.4.000266
6.   A. K. Bodukuri, K. Eswaraiah, K. Rajendar, and V. Sampath, *Perspect. Sci.*, **8**: 428 (2016); doi:10.1016/j.pisc.2016.04.096
7.   Q. C. Jiang, H. Y. Wang, B. X. Ma, Y. Wang, and F. Zhao, *J. Alloys Compd.*, **386**, Nos. 1−2: 177 (2005); doi:10.1016/j.jallcom.2004.06.015
8.   T. Schubert, B. Trindade, T. Weißgärber, and B. Kieback, *Mater. Sci. Eng. A*, **475**, Nos. 1−2: 39 (2008); doi:10.1016/j.msea.2006.12.146
9.   X. Wang, A. Jha, and R. Brydson, *Mater. Sci. Eng. A*, **364**, Nos. 1−2: 339, (2004); doi:10.1016/j.msea.2003.08.049
10.   B. Yang, F. Wang, and J. S. Zhang, *Acta Mater.*, **51**, No. 17: 4977 (2003); doi:10.1016/S1359-6454(03)00292-1
11.   J. Hashim, L. Looney, and M. S. J. Hashmi, *Journal of Materials Processing Technology*, **93**: 1 (1999).
12.   H. Uozumi *et al.*, *Mater. Sci. Eng. A*, **495**, Nos. 1−2: 282 (2008); doi:10.1016/j.msea.2007.11.088
13.   H. Hu, *Journal of Material Science*, **33**: 1579 (1998).
14.   M. Dhanashekar and V. S. Senthil Kumar, *Procedia Eng.*, **97**: 412 (2014); doi:10.1016/j.proeng.2014.12.265.9); E. J. Lavernia and N. J. Grant, *Mater. Sci. Eng. A*, **98**: 381 (1998).
15.   C. N. He, N. Q. Zhao, C. S. Shi, and S. Z. Song, *J. Alloys Compd.*, **487**, Nos. 1−2: 258 (2009); doi:10.1016/j.jallcom.2009.07.099
16.   P. Delhaes, *Carbon*, **40**, No. 5: 641 (2002); doi:10.1016/S0008-6223(01)00195-6
17.   R. S. Mishra and Z. Y. Ma, *Mater. Sci. Eng. R Reports*, **50**, Nos. 1−2: 1 (2005); doi:10.1016/j.mser.2005.07.001
18.   H. S. Arora, H. Singh, and B. K. Dhindaw, *Int. J. Adv. Manuf. Technol.*, **61**, Nos. 9−12: 1043 (2012); doi:10.1007/s00170-011-3758-8
19.   V. Sharma, U. Prakash, and B. V. M. Kumar, *J. Mater. Process. Technol.*, **224**: 117 (2015); doi:10.1016/j.jmatprotec.2015.04.019
20.   D. R. Ni, J. J. Wang, Z. N. Zhou, and Z. Y. Ma, *J. Alloys Compd.*, **586**: 368 (2014); doi:10.1016/j.jallcom.2013.10.013
21.   A. Thangarasu, N. Murugan, I. Dinaharan, and S. J. Vijay, *Arch. Civ. Mech. Eng.*, **15**, No. 2: 324 (2015); doi:10.1016/j.acme.2014.05.010
22.   M. Salehi, H. Farnoush, and J. A. Mohandesi, *Mater. Des.*, **63**: 419 (2014); doi:10.1016/j.matdes.2014.06.013
23.   B. W. Ahn, D. H. Choi, Y. H. Kim, and S. B. Jung, *Trans. Nonferrous Met. Soc. China (English Ed.)*, **22**, No. 3: s634 (2012); doi:10.1016/S1003-6326(12)61777-4
24.   M. Zohoor, M. K. BesharatiGivi, and P. Salami, *Mater. Des.*, **39**: 358 (2012); doi:10.1016/j.matdes.2012.02.042
25.   J. Guo, S. Amira, P. Gougeon, and X. G. Chen, *Mater. Charact.*, **62**, No. 9: 865 (2011); doi:10.1016/j.matchar.2011.06.007
26.   M. Yang, C. Xu, C. Wu, K. C. Lin, Y. J. Chao, and L. An, *J. Mater. Sci.*, **45**, No. 16: 4431 (2010); doi:10.1007/s10853-010-4525-1
27.   A. H. Feng and Z. Y. Ma, *Scr. Mater.*, **57**, No. 12: 1113 (2007); doi:10.1016/j.scriptamat.2007.08.020
28.   D. K. Lim, T. Shibayanagi, and A. P. Gerlich, *Mater. Sci. Eng. A*, **507**,

Nos. 1–2: 194 (2009); doi:10.1016/j.msea.2008.11.067

29. M. Gupta and M. L. Sharon Nai, *Magnesium, Magnesium Alloys, and Magnesium Composites* (J. Wiley and Sons, Inc.: 2010); doi:10.1002/9780470905098

30. B. R. Sunil, G. P. K. Reddy, H. Patle, and R. Dumpala, *J. Magnes. Alloy.*, **4**, No. 1: 52 (2016); doi:10.1016/j.jma.2016.02.001

31. R. S. Mishra, M. W. Mahoney, S. X. McFadden, N. A. Mara, and A. K. Mukherjee, *Scr. Mater.*, **42**, No. 2: 163 (1999); doi:10.1016/S1359-6462(99)00329-2

32. I. Dinaharan, N. Murugan, and S. Parameswaran, *Trans. Indian Inst. Met.*, **65**, No. 2: 159 (2012); doi:10.1007/s12666-012-0119-8

33. A. Dolatkhah, P. Golbabaei, M. K. Besharati Givi, and F. Molaiekiya, *Mater. Des.*, **37**: 458 (2012); doi:10.1016/j.matdes.2011.09.035

34. M. Zohoor, M. K. Besharati Givi, and P. Salami, *Mater. Des.*, **39**: 358 (2012); doi:10.1016/j.matdes.2012.02.042

35. A. Thangarasu, N. Murugan, I. Dinaharan, and S. J. Vijay, *Procedia Mater. Sci.*, **5**: 2115 (2014); doi:10.1016/j.mspro.2014.07.547

36. R. Bauri, G. D. Janaki Ram, D. Yadav, and C. N. Shyam Kumar, *Mater. Today Proc.*, **2**, Nos. 4–5: 3203 (2015); doi:10.1016/j.matpr.2015.07.115

37. V. V. Patel, V. Badheka, and A. Kumar, *Mater. Manuf. Process.*, **31**, No. 12: 1573 (2016); doi:10.1080/10426914.2015.1103868

38. M. Salehi, M. Saadatmand, and J. Aghazadeh Mohandesi, *Trans. Nonferrous Met. Soc. China (English Ed.)*, **22**, No. 5: 1055 (2012); doi:10.1016/S1003-6326(11)61283-1

39. N. Hoda, R. M. Singari, and V. J. Arulmoni, *International Journal of Research and Scientific Innovation (IJRSI)*, **III**: No. IX: 58 (2016).

40. R. Sathiskumar, N. Murugan, I. Dinaharan, and S. J. Vijay, *Mater. Des.*, **55**: 224 (2014); doi:10.1016/j.matdes.2013.09.053

41. S. Rathee, S. Maheshwari, A. N. Siddiquee, and M. Srivastava, *Crit. Rev. Solid State Mater. Sci.*, **43**, No. 4: 334 (2018); doi:10.1080/10408436.2017.1358146

42. K. Li, X. Liu, and Y. Zhao, *Coatings*, **9**, No. 2: (2019); doi:10.3390/COATINGS9020129

43. S. J. Vijay and N. Murugan, *Mater. Des.*, **31**, No. 7: 3585 (2010); doi:10.1016/j.matdes.2010.01.018

44. Y. N. Zhang, X. Cao, S. Larose, and P. Wanjara, *Can. Metall. Q.*, **51**, No. 3: 250 (2012); doi:10.1179/1879139512Y.0000000015

45. C. Moosbrugger, *ASM Int.*, **M**: 1 (2017); doi:10.1002/9780470905098.ch1

46. P. Asadi, G. Faraji, and M. K. Besharati, *Int. J. Adv. Manuf. Technol.*, **51**, Nos. 1–4: 247 (2010); doi:10.1007/s00170-010-2600-z

47. P. Asadi, M. K. Besharati Givi, and G. Faraji, *Mater. Manuf. Process.*, **25**, No. 11: 1219 (2010); doi:10.1080/10426911003636936

48. G. Faraji, O. Dastani, S. A. Asghar, and A. Mousavi, *Journal of Materials Engineering and Performance*, **20**: 1583 (2011); doi:10.1007/s11665-010-9812-0

49. D. Khayyamin, A. Mostafapour, and R. Keshmiri, *Mater. Sci. Eng. A*, **559**: 217 (2013); doi:10.1016/j.msea.2012.08.084

50. G. Faraji, O. Dastani, and S. A. A. Akbari Mousavi, *Proc. Inst. Mech. Eng. Part B J. Eng. Manuf.*, **225**, No. 8: 1331 (2011);

doi:10.1177/2041297510393584

51. D. Ahmadkhaniha, M. Heydarzadeh Sohi, A. Salehi, and R. Tahavvori, *J. Magnes. Alloy.*, **4**, No. 4: 314 (2016); doi:10.1016/j.jma.2016.11.002

52. M. Dadashpour, A. Mostafapour, R. Yeşildal, and S. Rouhi, *Mater. Sci. Eng. A*, **655**: 379 (2016); doi:10.1016/j.msea.2015.12.103

53. T. Chen, Z. Zhu, Y. Ma, Y. Li, and Y. Hao, *J. Wuhan Univ. Technol. Mater. Sci. Ed.*, **25**, No. 2: 223 (2010); doi:10.1007/s11595-010-2223-0

54. N. Singh, J. Singh, B. Singh, and N. Singh, *Mater. Today Proc.*, **5**, No. 9: 19976 (2018); doi:10.1016/j.matpr.2018.06.364

55. Y. Morisada, H. Fujii, T. Nagaoka, and M. Fukusumi, *Mater. Sci. Eng. A*, **433**, Nos. 1–2: 50 (2006); doi:10.1016/j.msea.2006.06.089

56. Y. Morisada, H. Fujii, T. Nagaoka, and M. Fukusumi, *Mater. Sci. Eng. A*, **419**, Nos. 1–2: 344 (2006); doi:10.1016/j.msea.2006.01.016

57. M. Azizieh, A. H. Kokabi, and P. Abachi, *Mater. Des.*, **32**, No. 4: 2034 (2011); doi:10.1016/j.matdes.2010.11.055

58. M. Azizieh, H. S. Kim, A. H. Kokabi, P. Abachi, and B. K. Shahraki, *Rev. Adv. Mater. Sci.*, **28**, No. 1: 85 (2011).

59. M. Srinivasan, C. Loganathan, V. Balasubramanian, Q. B. Nguyen, M. Gupta, and R. Narayanasamy, *Mater. Des.*, **32**, No. 3: 1672 (2011); doi:10.1016/j.matdes.2010.09.028

60. C. I. Chang, Y. N. Wang, H. R. Pei, C. J. Lee, X. H. Du, and J. C. Huang, *Key Eng. Mater.*, **351**: 114 (2007); doi:10.4028/0-87849-451-0.114

61. Y. Huang, T. Wang, W. Guo, L. Wan, and S. Lv, *Mater. Des.*, **59**, No. 8: 274 (2014); doi:10.1016/j.matdes.2014.02.067

62. M. Balakrishnan, I. Dinaharan, R. Palanivel, and R. Sivaprakasam, *J. Magnes. Alloy*, **3**, No. 1: 76 (2015); doi:0.1016/j.jma.2014.12.007

63. Y. Jiang, X. Yang, H. Miura, and T. Sakai, *Nano-SiO$_2$ Particles Reinforced Magnesium* (2013).

64. S. Sharma, A. Handa, S. S. Singh, and D. Verma, *Mater. Res. Express*, **6**, No. 12: (2019); doi:10.1088/2053-1591/ab54da

65. Y. Huang, T. Wang, W. Guo, L. Wan, and S. Lv, *Mater. Des.*, **59**, No. 8: 274 (2014); doi:10.1016/j.matdes.2014.02.067

66. M. Soltani, M. Shamanian, and B. Niroumand, *ADMT J.*, **8**, No. 1: 85 (2015).

67. M. Navazani and K. Dehghani, *Procedia Mater. Sci.*, **11**: 509 (2015); doi:10.1016/j.mspro.2015.11.082

68. B. Ratna Sunil, T. S. Sampath Kumar, U. Chakkingal, V. Nandakumar, and M. Doble, *J. Mater. Sci. Mater. Med.*, **25**, No. 4: 975 (2014); doi:10.1007/s10856-013-5127-7

69. S. Sharma, A. Handa, S. S. Singh, and D. Verma, *J. Magnes. Alloy*, **7**, No. 3: 487 (2019); doi:10.1016/j.jma.2019.07.001

70. S. Das, R. S. Mishra, K. J. Doherty, K. C. Cho, B. Davis, and R. DeLorme, *Frict. Stir Weld. Process. VII*, **3**: 245 (2016); doi:10.1007/978-3-319-48108-1_25

71. G. Vedabouriswaran and S. Aravindan, *J. Magnes. Alloy*, **6**, No. 2: 145 (2018); doi:10.1016/j.jma.2018.03.001

72. J. A. Del Valle, P. Rey, D. Gesto, D. Verdera, and O. A. Ruano, *Mater. Sci. Forum*, **706−709**: No. 1: 1823 (2012); doi:10.4028/www.scientific.net/MSF.706-709.1823

73.   C. J. Lee, J. C. Huang, and P. J. Hsieh, *Scr. Mater.*, **54**, No. 7: 1415 (2006);
      doi:10.1016/j.scriptamat.2005.11.056

74.   X. Du and B. Wu, *Sci. China, Ser. E Technol. Sci.*, **52**, No. 6: 1751 (2009);
      doi:10.1007/s11431-008-0210-x

75.   G. Madhusudhan Reddy, A. Sambasiva Rao, and K. Srinivasa Rao, *Trans.
      Indian Inst. Met.*, **66**, No. 1: 13 (2013); doi:10.1007/s12666-012-0163-4

76.   M. Abbasi, B. Bagheri, M. Dadaei, H. R. Omidvar, and M. Rezaei, *Int. J.
      Adv. Manuf. Technol.*, **77**, Nos. 9−12: 2051 (2015); doi:10.1007/s00170-014-
      6577-x

77.   J. Singh, Harvinder Lal, and N. Bala, *Int. J. Mech. Eng. & Rob. Res.*, **2**,
      No. 3: 271 (2013).

78.   H. S. Arora, H. Singh, B. K. Dhindaw, and H. S. Grewal, *Adv. Mater. Res.*,
      585: 579 (2012); doi:0.4028/www.scientific.net/AMR.585.579

79.   H. S. Arora, H. Singh, and B. K. Dhindaw, *Wear*, **303**, Nos. 1−2: 65 (2013);
      doi: 10.1016/j.wear.2013.02.023

80.   B. Ram, D. Deepak, and N. Bala, *Mater. Res. Express*, **6**, No. 2: (2019);
      doi:10.1088/2053-1591/aaf1e4

81.   M. Azizieh, A. N. Larki, M. Tahmasebi, M. Bavi, E. Alizadeh, and
      H. S. Kim, *J. Mater. Eng. Perform.*, **27**, No. 4: 2010 (2018);
      doi:10.1007/s11665-018-3277-y

82.   I. Dinaharan, S. C. Vettivel, M. Balakrishnan, and E. T. Akinlabi, *J. of
      Magnesium and Alloys*, **7**, Iss. 1: 155 (2019);
      https://doi.org/10.1016/j.jma.2019.01.003

83.   G. Faraji and P. Asadi, *Mater. Sci. Eng. A*, **528**, No. 6: 2431 (2011);
      doi:10.1016/j.msea.2010.11.065

84.   D. Lu, Y. Jiang, and R. Zhou, *Wear*, **305**, Nos. 1−2: 286 (2013);
      doi:10.1016/j.wear.2012.11.079

85.   S. H. Whang et al., *Nanostructured Metals and Alloys* (2011), pp. XIV−
      XIX; doi:10.1016/b978-1-84569-670-2.50027-7

86.   C. S. Pande and K. P. Cooper, *Prog. Mater. Sci.*, **54**, No. 6: 689 (2009);
      doi:10.1016/j.pmatsci.2009.03.008

87.   Y. S. Sato, M. Urata, H. Kokawa, and K. Ikeda, *Mater. Sci. Eng. A*, **354**,
      Nos. 1−2: 298 (2003); doi:10.1016/S0921-5093(03)00008-X

88.   P. Xiao, Y. Gao, C. Yang, Z. Liu, Y. Li, and F. Xu, *Mater. Sci. Eng. A*, **710**,
      No. 10: 251 (2017); doi:10.1016/j.msea.2017.10.107

89.   Y. P. Hung, J. C. Huang, K. J. Wu, and C. Y. A. Tsao, *Mater. Trans.*, **47**,
      No. 8: 1985 (2006); doi:10.2320/matertrans.47.1985

90.   Z. Zhang and D. L. Chen, *Mater. Sci. Eng. A*, **483−484**, Nos. 1−2: 148
      (2008); doi:10.1016/j.msea.2006.10.184

91.   A. Sanaty-Zadeh, *Mater. Sci. Eng. A*, **531**: 112 (2012);
      doi:10.1016/j.msea.2011.10.043